Amorphous TeO_2 as P-type Oxide Semiconductor for BEOL Devices

John Robertson[1*], X Zhang[1], Q Gui[2], Y Guo[2]

[1] Engineering Dept, Cambridge University, Cambridge CB3 0FA, UK
[2] Wuhan University, Wuhan 430072, China
E-mail: jr214@cam.ac.uk

Back-end-of-line devices need amorphous dopable bipolar oxide semiconductors. However, there are no practical p-type oxides, they are layered, require high processing temperatures or ineffective due to self-compensation by native defects. TeO_2 is a glass. Our simulations find that amorphous (a-) TeO_2 is chemically ordered, can be degenerately doped p-type, does not self-compensate and uses low-cost processable materials.

There is presently an intensive search for practical back-end-of-line (BEOL) oxides that can be doped n- or p-type. There are many n-type oxides like InGaZn oxide. However, there are no low-cost p-type oxides with hole mobility. Compounds like $CuAlO_2$ do not favor disorder due to their layered structure [1], $ZnRh_2O_4$ uses high-temperature refractory metals [2], while SnO is p-type but its 0.7eV indirect gap causes large leakage currents [3]. Ternary oxides like $SnTa_2O_6$ have wider gaps [4] but their dopability is limited by intrinsic oxygen vacancies V_O^{2+}, a key factor that is rarely tested [5-8]. β-TeO_2 has a high hole mobility (3000 cm^2/V.s, calculated [9]), ~300 cm^2/V.s experimental [10) due to s-like upper valence band [9-11].

We show here that a-TeO_2 can be doped p-type and can be structurally disordered without suffering V_O^{2+} self-compensation, making it the first viable p-type oxide semiconductor.

The electronic structures of rutile and layered (β- or α-) phases of TeO_2 are calculated by density functional theory (GGA) and with HSE hybrid functional bandgap corrections. Electron affinity (EA) and ionization potential (IP) energies below the vacuum level are found using a supercell with a 15Å vacuum spacing. Defect compensation is calculated from the defect formation energy ΔH_q [5]

$$\Delta H_q(\mu,E_f) = E_q - E_H + q\Delta E_f + \Sigma n_\alpha \mu_\alpha$$

as a function of the host total energy E_H, the defect charge (q), and the Fermi energy (E_f) with respect to the valence band edge, n_α is the number of atoms of element α and μ_α is the chemical potential of α.

The amorphous oxide is studied by ab-initio molecular dynamics (AIMD) for a 120-atom crystalline cell heated to 2000K for 4ps, cooled to 300K, and then relaxed at 300K for 5 ns. Doped oxide, not yet studied, is modeled by substituting two As_{Te} sites, to avoid needing spin polarisation.

β-TeO_2 is a quasi-layer compound, with an orthorhombic structure, stabilized from its rutile-TeO_2 phase by a 0.2 eV per formula unit (fu), Fig. 1, Table 1. Fig. 2(a,b) compares the HSE band structures of β-TeO_2 and rutile-TeO_2. The EA and IP of β-TeO_2 for bulk cells are found to be 3.16 eV and 6.45 eV respectively, consistent with previous studies [10,12]. There is a direct 3.3 eV bandgap at Γ and a shallow Te s-like valence band maximum (Fig. 3), giving a small hole mass and high theoretical hole mobility.

Fig. 4(a) shows a structural model of a-TeO_2 by AIMD. Locally, it resembles β-TeO_2, with 4-fold Te sites and 2-fold O sites. The O bridges are not always grouped in bridge pairs. Fig. 5(b) shows the radial distribution function (RDF) of this disordered TeO_2. The first neighbor peak due to heteropolar Te-O bonds occurs at 1.96 Å, with second neighbor peaks at 2.8Å due to O-O bonds and 3.8Å peak from Te-Te bonds, as earlier [12]. There are no first-neighbor homopolar bonds. Thus, although O and Te are both chalcogens, their sizable electronegativity difference strongly favors heteropolar bonding. Hence, the chemical ordering of a-TeO_2 is quite similar to that in β-TeO_2, while allowing structural disorder to occur. Previously a notable type of disorder was due to varying the number of long (non-covalent) Te-O bonds [13]

Fig 5 shows the calculated defect formation energies ΔH of the oxygen vacancy V_O for O-poor and O-rich β-TeO_2, where V_O is the principal compensating defect. We see that ΔH of V_O^{2+} crosses the 0 eV axis below the valence band edge, ie. ΔH is positive within the gap, so these defects are endothermic and they do not cause self-compensation. Other defects, the interstitials I_O, I_{Te} and vacancy V_{Te} are less problem.

Fig. 6 compares the calculated absolute EA and IP values to the estimated doping limits of oxides [6]. The IP of β-TeO_2 is close to the doping limit for p-type oxides. However, these limits apply best if the compensating defect is a V_O defect in an ionic lattice. TeO_2 is a mainly covalent Te-O-Te network, and this pushes the lower doping limit downwards somewhat.

Although self-compensation is the key aspect, it is critical to test the actual dopability of a-TeO_2 directly by creating substitutional dopant sites like As_{Te} or Sb_{Te}. In Fig. 7, we insert two As atoms into a AIMD supercell and find that E_F lies at the valence band edge of a-TeO_2. Thus, TeO_2:As differs from Ga_2O_3 with its deep acceptors. This is a useful test. Zavabeti [10] studied the undoped oxide experimentally but not the doped oxide. These still need a check experimentally. It is interesting that TeO_2 is unusual that it can be shallow doped p-type by N of the O site, in contrast to ZnO or Ga_2O_3.

We have calculated the key factors needed to test defect self-compensation and disorder tolerance for a-TeO_2 to be classed as a viable p-type semiconductor for BEOL devices.

References

[1] H Kawazoe et al, Nature 389 030 (1997).
[2] H Hosono, Jpn J App Phys 52 090001 (2013)
[3] Y Ogo et al, App Phys Let 93 032113 (2008)
[4] Y Hu et al, Chem Mats 33 212 (2021)
[5] A Zunger, App Phys Let 83 57 (2003)
[6] J Robertson, S J Clark, Phys Rev B 83 075205 (2011)
[7] Z Zhang, Y Guo, J Robertson, Chem Mats 34 643 (2022)
[8] M Barone, et al, J Phys Chem C 126 3764 (2022)
[9] S Guo, et al, Nanoscale 10 8397 (2018)
[10] A Zavabeti et al, Nature Electronics 4 277 (2021)
[11] J Shi et al, App Phys Let 122 101901 (2023)
[12] F Pietrucci, S Caravati, M Bernasconi, Phys Rev B 78 064203 (2008)
[13] O L G Alderman et al, J Phys Chem Let 11 427 (2020)

Table 1.: Comparison of rutile, α-, and β-TeO_2.

	rutile-TeO_2	α-TeO_2	β-TeO_2
Symmetry	$P4_2/mnm$	$P4_12_12$	P_{bca}
Crystal system	Rutile	Distorted rutile	Ortho-rhombic
E_{form} eV/f.u	-1.27	-1.49	-1.49
Gap (eV) (HSE)	0.72	2.65	3.29
IP (eV) (HSE)	6.09	7.31	6.45
EA (eV) (HSE)	5.37	4.66	3.16
Band gap	indirect	indirect	direct

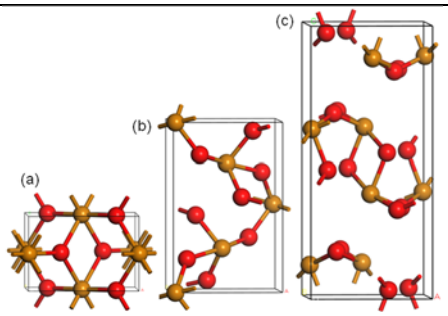

Fig. 1(a) rutile TeO_2, (b) α-TeO_2, (c) β-TeO_2

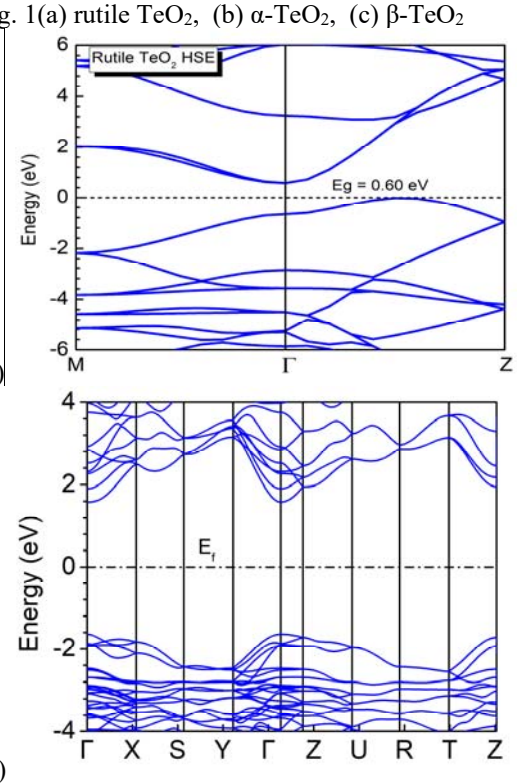

Fig. 2. HSE Bands of (a) rutile TeO_2, (b) β-TeO_2.

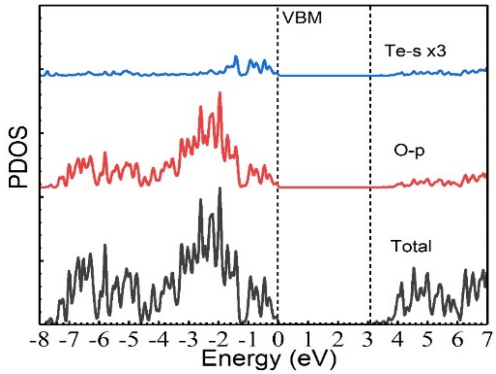

Fig. 3. Partial density of states (PDOS) of β-TeO_2

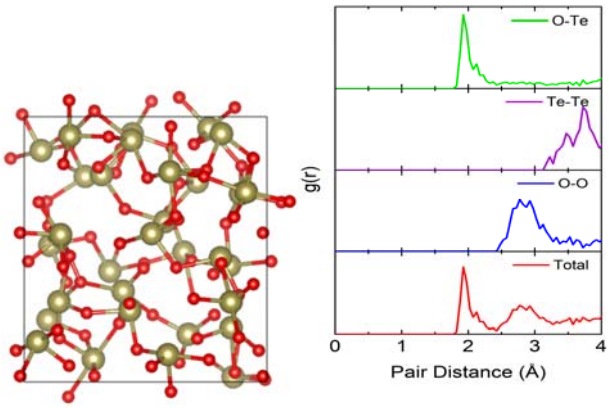

Fig 4(a). Structural model of a-TeO_2 by AIMD and (b) calculated RDF of this model.

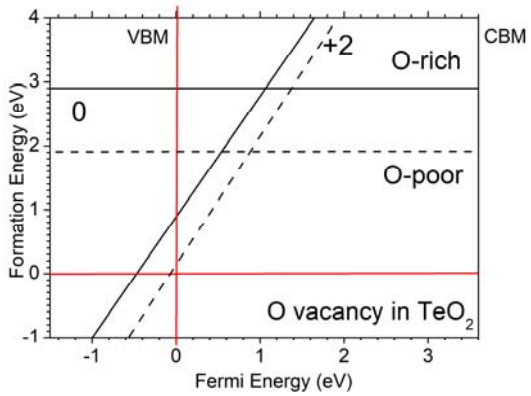

Fig 5 Defect formation energy vs.Fermi energy, for V_O self-compensation for O-rich and O-poor β-TeO_2.

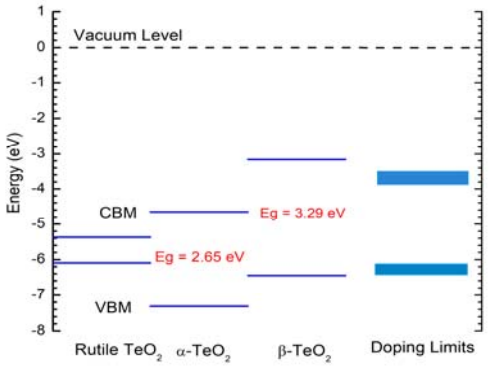

Fig. 6: Band-edge energies of TeO_2 phase vs. vacuum level, compared to approximate doping-limit energies [7].

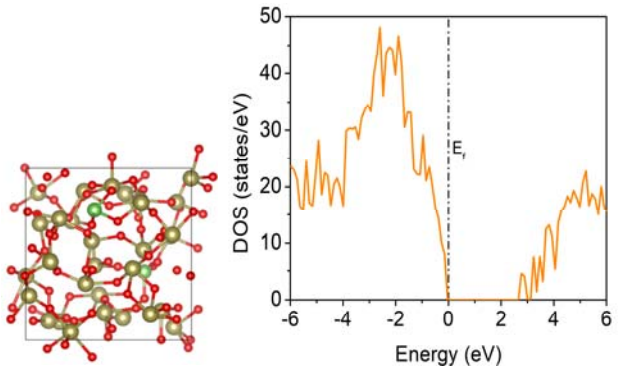

Fig. 7(a) network structure and (b) DOS with two As_{Te} acceptor sites, showing shallow doping in a-TeO_2 with E_F at the valence band edge.